JOC*Article*

The Photochemistry of 4-Azidopyridine-1-oxide

Katherine J. Hostetler, Kyle N. Crabtree, and James S. Poole*

Department of Chemistry, Ball State University, Muncie, Indiana 47306

jspoole@bsu.edu

Received June 19, 2006

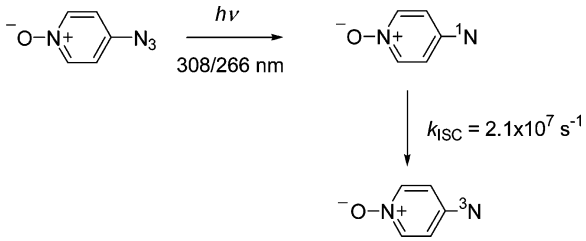

Laser flash photolysis of 4-azidopyridine-1-oxide at 266 or 308 nm yields triplet 4-nitrenopyridine-1-oxide as the dominant reactive intermediate species, with k_{ISC} of approximately 2×10^7 s^{-1}. No evidence of products arising from the singlet nitrene was observed, indicating a slow rate of cyclization to the benzazirine and didehydroazepine species. The slow rate of cyclization is postulated to be due to the aminoxyl-like electronic configuration of this species, which withdraws spin density from sites for potential cyclization.

Introduction

The chemistry of azidoheterocyclic-*N*-oxides has been investigated in the literature due to the potential of these compounds as antitumor agents.[1,2] More recently, the potential of these reagents as sources of nitrene species was studied by product analysis following thermolysis or photolysis of the azides in the presence of nucleophiles.[3] In general terms, it was found that the product distributions arising from thermolysis and photolysis of both 3- and 4-azidopyridine-1-oxides were complex, and not readily resolved. The thermo- and photochemical reactions of the 2-azido analogues of these compounds follow significantly different reaction paths to generate 2-cyanopyrroles.[4]

We have chosen to study the chemistry of azidoheterocyclic-*N*-oxides using nanosecond laser flash photolysis (LFP) and time-resolved infrared (TRIR) techniques in order to elucidate the nature of the nitrene intermediates and perhaps clarify the product analysis studies of prior workers.[3] In this contribution, we report the results of our studies on an archetypal system, 4-azidopyridine-1-oxide (**1**). 4-Azidopyridine-1-oxide was chosen for our initial study due to the fact that its molecular symmetry afforded us with the simplest of these types of systems. If photolysis of the azido group proceeds in the same manner as other aryl azides,[5,6] we would expect the reactions shown in Scheme 1.

Alternative reaction paths involving the photoactive *N*-oxide group are also possible, but it is known that photolysis of aromatic azides proceeds with reasonable quantum yield.[7]

Experimental Methods

Compound **1** was prepared from the corresponding hydrazine,[8] using the method of Itai and Kamiya,[1] and recrystallized from acetone (see Supporting Information). All solvents used in this study (including pyridine) were obtained in spectroscopic purity from commercial sources and were used without additional purification. Diethylamine was purified by distillation, stored over KOH, and used as soon after distillation as possible. The instruments used

(1) Itai, T.; Kamiya, S. *Chem. Pharm. Bull.* **1961**, *9*, 87.
(2) (a) Itai, T.; Kamiya, S. *Chem. Pharm. Bull.* **1963**, *11*, 348. (b) Itai, T.; Kamiya, S. *Chem. Pharm. Bull.* **1963**, *11*, 1059.
(3) Abramovitch, R. A.; Bachowska, B.; Tomasik, P. *Pol. J. Chem.* **1984**, *58*, 805.
(4) Abramovitch, R. A.; Cue, B. W., Jr. *J. Org. Chem.* **1973**, *38*, 173. (b) Abramovitch, R. A.; Cue, B. W., Jr. *J. Am. Chem. Soc.* **1976**, *98*, 1478.
(5) Platz, M. S. In *Reactive Intermediate Chemistry*; Moss, R. A., Platz, M. S, Jones, M. J., Eds.; John Wiley & Sons Inc.: Hoboken, NJ, 2004; pp 522−545. (b) Borden, W. T.; Gritsan, N. P.; Hadad, C. M.; Karney, W. L.; Kemnitz, C. R.; Platz, M. S. *Acc. Chem. Res.* **2000**, *33*, 765. (c) Gritsan, N. P.; Zhu, Z.; Hadad, C. M.; Platz, M. S. *J. Am. Chem. Soc.* **1999**, *121*, 1202.
(6) Gritsan, N. P.; Likhotvoric, I.; Tsao, M.-L.; Celibi, N.; Platz, M. S.; Karney, W. L.; Kemnitz, C. R.; Borden, W. T. *J. Am. Chem. Soc.* **2001**, *123*, 1425. (b) Gritsan, N. P.; Tigelaar, D.; Platz, M. S. *J. Phys. Chem. A* **1999**, *103*, 4465.
(7) Leyshon, L. J.; Reiser, A. *J. Chem. Soc., Faraday Trans. 2*, **1972**, 1918. (b) Go, C. L.; Waddell, W. H. *J. Org. Chem.* **1983**, *48*, 2897.
(8) Katritzky, A. R. *J. Chem. Soc. Abstr.* **1956**, 2404.

10.1021/jo061259o CCC: $33.50
Published on Web 10/21/2006

SCHEME 1. Potential Reactions Following Photolysis of 4-Azidopyridine-1-oxide (1)

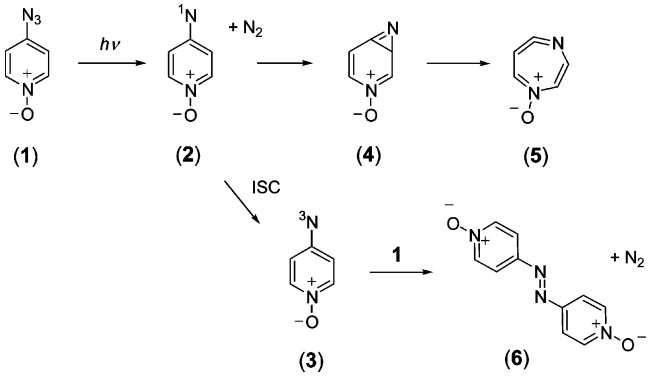

for characterization of organic compounds are described in the Supporting Information.

The Laser flash photolysis system utilized at The Ohio State University has been described previously.[9] A solution of **1** (2−3 mL), in an appropriate solvent, was deoxygenated using a thin stream of bubbling argon over a period of at least 10 min. The solvents used in this component of the study were 3-methylpentane, dichloromethane, acetonitrile, and pyridine. The concentration of solution for most experiments was chosen to give an optical density of approximately 1.5−2.0 at 308 nm, except in the cases of experiments where the concentration of **1** had to be varied in order to yield kinetic information: in such cases the optical density was varied between 0.5 and 2.5. Samples were irradiated using a Xe−Cl excimer laser (308 nm, nominal pulse width = 30 ns, 50 mJ/pulse), and the transient absorbance signals captured by CCD (for transient spectra) or fast photomultiplier (for kinetic traces).

The sub-microsecond time-resolved infrared (TRIR) laser flash photolysis system used at The Ohio State University has also been described previously.[10] In the TRIR experiment, a solution of **1** (3−10 mM in a 6−10 mL reservoir) in h_3- or d_3-acetonitrile was pumped through a 0.5 mm path length BaF_2 flow cell. The sample was irradiated at 266 nm, using an Nd:YAG laser (50 Hz repetition rate, 0.5 mJ/pulse). Signal collection was achieved using a dispersive infrared spectrometer (broadband $MoSi_2$ source, resolution approximately 16 cm^{-1}).

Theoretical Calculations

Density functional theory (DFT) calculations were performed using the GAUSSIAN 03 program suite.[11] Geometry optimizations and energies were performed at the B3LYP/6-31G* level of theory for all species,[12] and vibrational frequencies were calculated at the same level of theory, corrected by factors of 0.9614 (frequencies), 0.9806 (zero-point energies), and 0.9989 (enthalpic corrections to 298 K) as recommended by Scott and Radom.[13] Transition states for nitrene and azide rearrangements were found to have a single imaginary frequency, corresponding to the appropriate reaction coordinate. Natural population analysis (NPA)[14] was performed on critical intermediates. The relative energetics of **2** and **3** were further refined using CASSCF calculations up to the CAS(10,9)/6-31G* level of theory.[15]

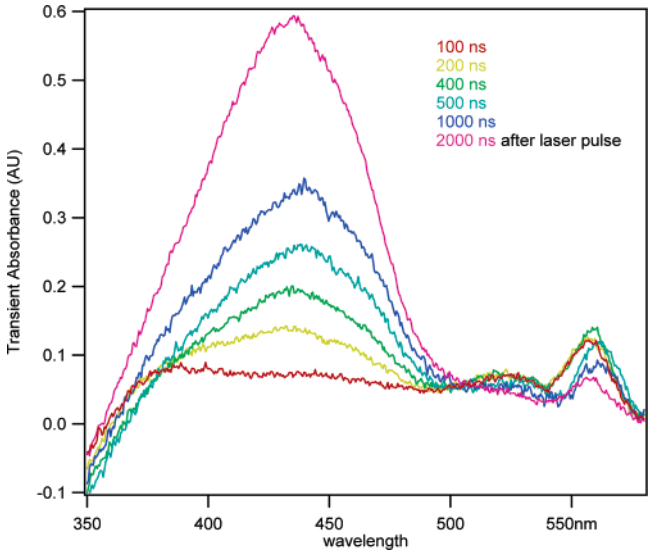

FIGURE 1. Transient spectra obtained following 308 nm laser flash photolysis of **1** (0.07 mM) in 3-methylpentane at 298 K. Each spectrum is obtained over a 10 ns time interval.

Results

Laser Flash Photolysis. Room temperature irradiation of **1** in 3-methylpentane at 308 nm yielded the transient spectra shown in Figure 1. The spectra show two temporally distinct features—a partially structured band with maxima at 523 and 557 nm, and a broader feature with an absorbance maximum at 435 nm. The 523 and 557 nm signals decay at the same rate (within experimental uncertainty, Figure 2), leading us to believe that the same transient species is responsible for both signals. The bands at 520−560 nm are assigned to the triplet nitrene (**3**). Such an assignment is consistent with other triplet arylnitrene spectra, although somewhat more intense than usual for simple aryl nitrenes,[5,6] but not necessarily for more complex heteroarylnitrenes.[16] The growth rate of the signal at 557 nm could also be measured at small timescales (Figure 2 inset).

(9) For example, see Martin, C. B.; Shi, X.; Tsao, M.-L.; Karweik, D.; Brooke, J.; Hadad, C. M.; Platz, M. S.; *J. Phys. Chem. B* **2002**, *106*, 10263. Temperature control was achieved by utilizing the quartz cryostat/thermostabilized nitrogen stream system described in ref 5c.

(10) For example, see: Martin, C. B.; Tsao, M-L.; Hadad, C. M.; Platz, M. J. *J. Am. Chem. Soc.* **2002**, *125*, 7226.

(11) Frisch, M. J.; Trucks, G. W.; Schlegel, H. B.; Scuseria, G. E.; Robb, M. A.; Cheeseman, J. R.; Montgomery, J. A., Jr.; Vreven, T.; Kudin, K. N.; Burant, J. C.; Millam, J. M.; Iyengar, S. S.; Tomasi, J.; Barone, V.; Mennucci, B.; Cossi, M.; Scalmani, G.; Rega, N.; Petersson, G. A.; Nakatsuji, H.; Hada, M.; Ehara, M.; Toyota, K.; Fukuda, R.; Hasegawa, J.; Ishida, M.; Nakajima, T.; Honda, Y.; Kitao, O.; Nakai, H.; Klene, M.; Li, X.; Knox, J. E.; Hratchian, H. P.; Cross, J. B.; Adamo, C.; Jaramillo, J.; Gomperts, R.; Stratmann, R. E.; Yazyev, O.; Austin, A. J.; Cammi, R.; Pomelli, C.; Ochterski, J. W.; Ayala, P. Y.; Morokuma, K.; Voth, G. A.; Salvador, P.; Dannenberg, J. J.; Zakrzewski, V. G.; Dapprich, S.; Daniels, A. D.; Strain, M. C.; Farkas, O.; Malick, D. K.; Rabuck, A. D.; Raghavachari, K.; Foresman, J. B.; Ortiz, J. V.; Cui, Q.; Baboul, A. G.; Clifford, S.; Cioslowski, J.; Stefanov, B. B.; Liu, G.; Liashenko, A.; Piskorz, P.; Komaromi, I.; Martin, R. L.; Fox, D. J.; Keith, T.; Al-Laham, M. A.; Peng, C. Y.; Nanayakkara, A.; Challacombe, M.; Gill, P. M. W.; Johnson, B.; Chen, W.; Wong, M. W.; Gonzalez, C.; Pople, J. A.; *Gaussian 03*, Revision C.02; Gaussian, Inc.: Wallingford, CT, 2004.

(12) (a) Becke, A. D. *Phys. Rev. A* **1988**, *38*, 3098. (b) Becke, A. D. *J. Chem. Phys.* **1993**, *98*, 5648. (c) Lee, C.; Yang, W.; Parr, R. G. *Phys. Rev. B* **1988**, *37*, 785.

(13) Scott, A. P.; Radom, L. *J. Phys. Chem.* **1996**, *100*, 16502.

(14) (a) Reed, A. E.; Weinstock, R. B.; Weinhold, F. *J. Chem. Phys.* **1985**, *83*, 735. (b) Reed, A. E.; Weinhold, F.; Curtiss, J. A. *Chem. Rev.* **1988**, *88*, 899.

(15) (a) Karney, W. L.; Borden, W. T. *J. Am. Chem. Soc.* **1997**, *119*, 1378. (b) Johnson, W. T. G.; Sullivan, M. B.; Cramer, C. J. *Int. J. Quantum Chem.* **2001**, *85*, 492.

(16) Cerro-Lopez, M.; Gritsan, N. P.; Zhu, Z.; Platz, M. S. *J. Phys. Chem. A* **2000**, *104*, 9681.

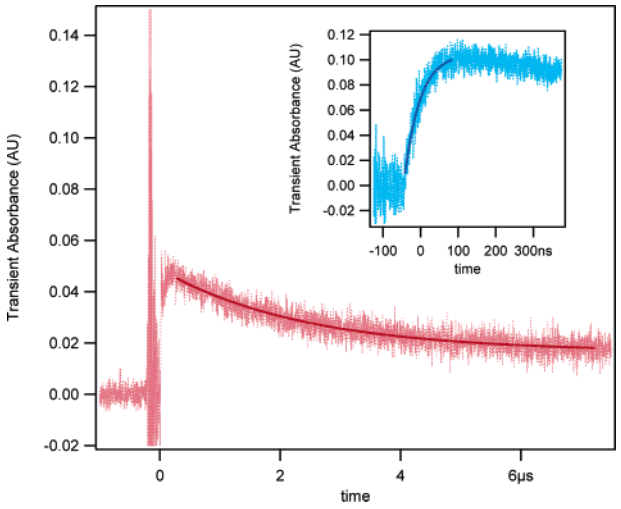

FIGURE 2. Decay of signal at 557 nm following 308 nm LFP of **1** (0.07 mM) in 3-methylpentane at 298 K. Inset: Short time scale growth of signal at 557 nm following LFP of **1** in 3-methylpentane. Signals were averaged over four acquisitions each

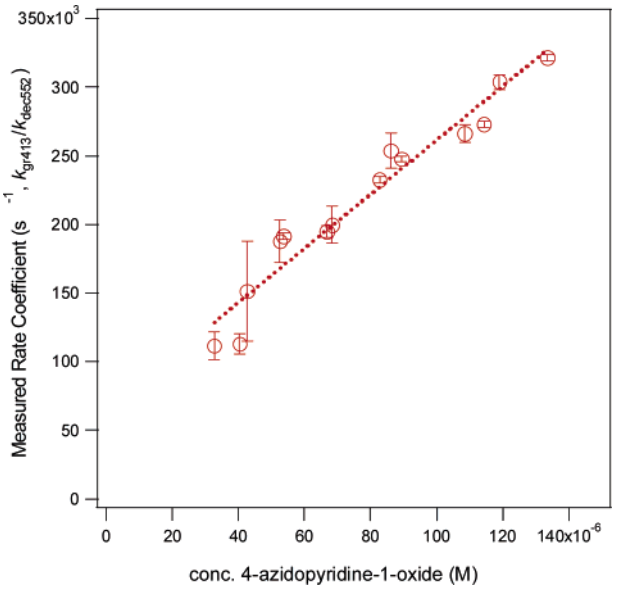

FIGURE 3. Dependence of the rate of decay of triplet nitrene signal (**3**, 552 nm) and/or rate of growth of **6** (413 nm) on the solution concentration of **1** (pseudo-first-order kinetic plot).

The growth rate was found to be independent of the starting azide concentration and some 2 orders of magnitude greater than the decay rate for the signal at 557 nm. Therefore, to reasonable approximation, the growth and decay rates for this signal were treated as being temporally separable. It is further assumed that, like other arylnitrenes, the triplet species is generated by intersystem crossing from the nitrene singlet state, rather than from an azide triplet state.[17] Thus, the observed rate coefficient for intersystem crossing (k_{ISC}) from the singlet nitrene was determined to be $(2.14 \pm 0.08) \times 10^7$ s^{-1}, a value that lies in the range of values reported for substituted phenylnitrenes.[5,6]

The feature at 435 nm has a growth rate which was demonstrated to be dependent on the starting concentration of azide and the same (within experimental uncertainty) as the decay rate for the triplet (Figures 2 and 3). In addition, this signal did not decay within the longest observable timebase of the instrument. On this basis, we have assigned the signal at 435 nm to the compound 4,4′-azo-bis(pyridine-1-oxide), **6**. It is noteworthy that the spectra obtained in 3-methylpentane remain unchanged with the addition of 0.5 M diethylamine to solution, further evidence against the formation of **5**, which would be rapidly trapped to form the azepine product.[18]

Photolysis of 4-azido-pyridine-1-oxide in dichloromethane at 298 K yielded transient spectra that are effectively the same as those shown in Figure 1, except that the absorbances of the azo-compound are shifted (Table 1). The significant solvatochromic behavior of compound **6** has been reported previously and is consistent with our observations.[19] An interesting difference between the two experiments is the presence of a very weak and short-lived transient signal observable at 493 nm in dichloromethane. The rate of decay for the signal at 493 nm is $(1.9 \pm 0.3) \times 10^7$ s^{-1}, in reasonable agreement with the growth rate measured for the signal at 554 nm, $(2.41 \pm 0.08) \times 10^7$ s^{-1}. On this basis, we tentatively assign the signal at 493 nm to the singlet nitrene, **2**.

In order to further confirm our assignment of spectral peaks to the triplet (**3**) and azo-dimer (**6**), we measured the growth rate of the signal at 554 nm in dichloromethane as a function of temperature. The LFP signal was obtained over a temperature range of 179−298 K, and the value of k_{ISC} varied by less than 10% over this range, effectively temperature independent, as would be expected for an intersystem crossing process.[5,6] In addition, the observed value for k_{ISC} at 298 K is not strongly dependent on solvent polarity (Table 1).

The dependence of decay kinetics of the 554 nm signal was also measured as a function of azide concentration (Figure 3) and, as expected, exhibited nonlinear behavior at low concentrations. Regression analysis of the linear (pseudo-first-order) region of the curve yielded a rate coefficient for the triplet nitrene-azide coupling reaction of $k_C = (1.96 \pm 0.13) \times 10^9$ M^{-1} s^{-1} in dichloromethane at 298 K. This compares with the slightly higher value obtained in 3-methylpentane at 298 K (Table 1).

Attempts to observe quenching of the triplet signal in the presence of oxygen were unsuccessful. LFP of a solution of **1** (0.13 mM) in dichloromethane in the presence and absence of oxygen showed only a marginal increase in the observed decay rate of the 554 nm signal in the presence of oxygen (Table 1), but since both derived second-order rate coefficients lie within the experimental uncertainty of the rate coefficient for dimerization over a range of concentrations of **1** (0.02−0.14 mM), it seems unlikely that oxygen trapping of **3** competes with dimerization to any significant extent.

Attempts to observe the pyridine-nitrene ylide **7** were

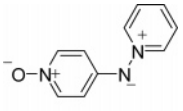

(**7**)

unsuccessful − photolysis of **1** in neat pyridine at 298 K

(17) Marcinek, A.; Leyva, E.; Whitt, D.; Platz, M. S. *J. Am. Chem. Soc.* **1993**, *115*, 8609.

(18) (a) DeGraff, B. A.; Gillespie, D. W.; Sundberg, R. J. *J. Am. Chem. Soc.* **1974**, *96*, 7491. (b) Li, Y.-Z.; Kirby, J. P.; George, M. W.; Poliakoff, M.; Schuster, G. B. *J. Am. Chem. Soc.* **1998**, *110*, 8092.

(19) Muniz-Miranda, M.; Pergolese, B.; Sbrana, G.; Bigotto, A. *J. Mol. Struct.* **2005**, *744−747*, 339.

TABLE 1. Kinetic Data for Photochemistry (Laser Flash Photolysis) of 4-Nitrenopyridine-1-oxide

solvent	λ_{max}(**2**) (nm)	λ_{max}(**3**) (nm)	λ_{max}(**6**) (nm)	k_{ISC} (10^7 s^{-1})	k_C (10^9 M^{-1} s^{-1})
3-methylpentane	not obs.	523, 557	435	2.40 ± 0.07	5.6 ± 0.4[a] 5.0 ± 0.5[b]
3-methylpentane + 0.5 M $HNEt_2$		523, 559	438		
dichloromethane	493	522, 554	417	2.23 ± 0.04	1.96 ± 0.13[c] 1.86 ± 0.01[d]
dichloromethane + O_2					1.96 ± 0.01[d]
dichloromethane + 0.5 M $HNEt_2$		521, 555	420		
acetonitrile	not obs.	517, 547	415	2.49 ± 0.05	2.3 ± 0.1[e]
pyridine	not obs.	526, 557	427		

[a] Measured from signal decay at 557 nm. [b] Measured from signal growth at 435 nm. [c] Determined from combined data for decay at 554 nm and growth at 417 nm. [d] Determined from decay at 417 nm at a single concentration of **1**. [e] Estimated from growth at 415 nm and decay at 547 nm at a single concentration of **1** in acetonitrile

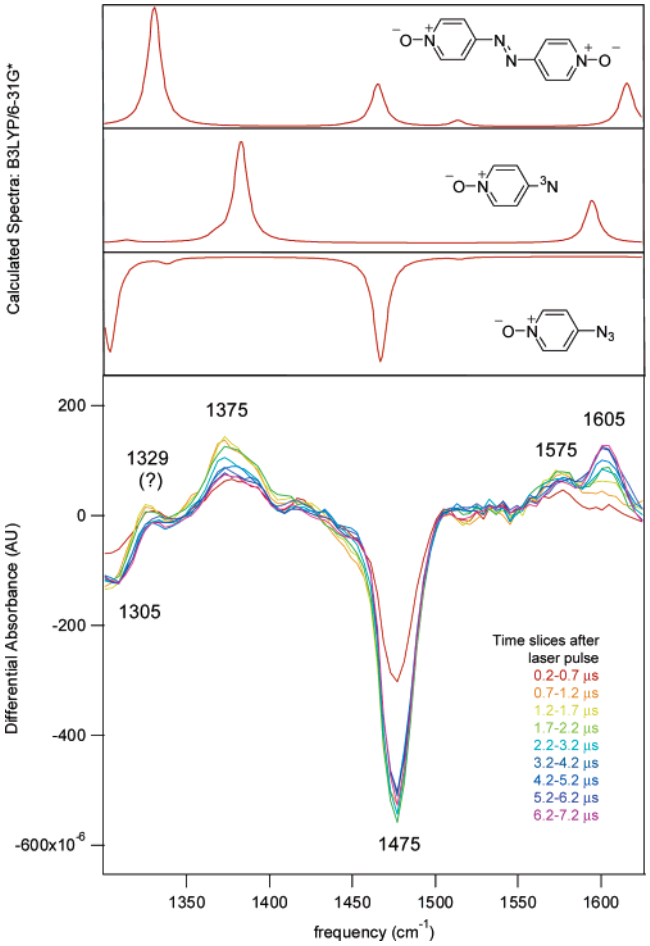

FIGURE 4. Top half: simulated differential IR spectra for disappearance of **1** and appearance of **3** and **6**, based on calculated vibrational frequencies. Bottom half: transient differential IR spectra (time slices) following 298 K irradiation of a d_3-acetonitrile solution of **1** (5 mM), at 266 nm. Experimental spectra have been smoothed for reasons of clarity.

generated spectra that were qualitatively similar to those generated in 3-methylpentane and dichloromethane, the only quantitative change in absorbance maxima for **3** and **6** due to solvatochromic shifts (Table 1).

Time-Resolved Infrared Spectroscopy. Irradiation of a solution of **1** in d_3-acetonitrile yielded the transient differential spectra shown in Figure 4. The differential spectra observed are consistent with the simulated spectra for the bleaching of **1** and the formation of **3** and **6**. The simulated spectra in Figure 4 were determined computationally at the B3LYP/6-31G* level of theory for the isolated species (i.e., no solvent).

On the basis of the spectra in Figure 4, the kinetics of the signals at 1370 (assigned to **3**) and 1600 (assigned to **6**) cm^{-1} were investigated (Figure 5). Attempts to obtain kinetic data for the signals at 1329 (**6**) and 1575 (**3**) cm^{-1} were unsuccessful: the former due to spectral interference arising from bleaching of the azide at 1305 cm^{-1}, the latter due to spectral interference due to partial overlap of the feature at 1600 cm^{-1}.

The TRIR signal at 1370 cm^{-1} shows a rapid growth, followed by a considerably slower decay. The growth kinetics for this signal cannot be reliably determined due to the time scale constraints of the instrumental method, but it is estimated to be of the order 10^7 s^{-1}—broadly consistent with ISC rate coefficients measured by LFP. The observed first-order rate constant for the decay of the signal was determined to be (7.6 ± 1.1) × 10^6 s^{-1}, which based on a concentration for **1** of about 4−5 mM (and assuming pseudo-first-order kinetics) gives a value for the second-order rate coefficient of reaction of **3** with **1** which is consistent with the value obtained from UV−visible LFP studies (1.5 × 10^9 M^{-1} s^{-1}). What is most important to note is that the rate coefficient for the growth of signal at 1600 cm^{-1} (corresponding to the formation of **6** from **1** and **3**) has the same value, within the limits of experimental uncertainty.

An additional study of the region 1900−1700 cm^{-1} following laser excitation of **1** in h_3-acetonitrile solution showed no discernible signals. Calculated vibrational spectra of the didehydroazepine (or ketenimine) **5** indicate that this species should have a diagnostic absorbance at 1881 cm^{-1} and that the benzazirine **4** should have an absorbance at 1744 cm^{-1}. The absence of these signals indicates that singlet nitrene chemistry plays a relatively minor role in the overall photochemistry of **1**.

Product Analysis. HPLC analysis of solutions of **1** photolyzed under argon show only two significant peaks, one corresponding to the starting material **1** and the other to **6**. No other peaks were observed to any significant degree. Similarly, ^1H NMR spectra of the d_3-acetonitrile solution shows only two compounds to any significant extent. The primary photoproduct was isolated, and confirmed to be the azo-compound **6**.

Theoretical Calculations. Calculations were performed at the B3LYP/6-31G* level of theory for 4-nitrenopyridine-1-oxide, 4-pyridylnitrene, and phenylnitrene (as a comparator) to determine the relative energies of the species **2**, **3**, **4**, and **5** (and their analogues), as well as the transition states leading to the formation of these species where applicable. In addition, calculations for species arising from *N*-oxide chemistry were also performed, specifically those arising from cyclization of

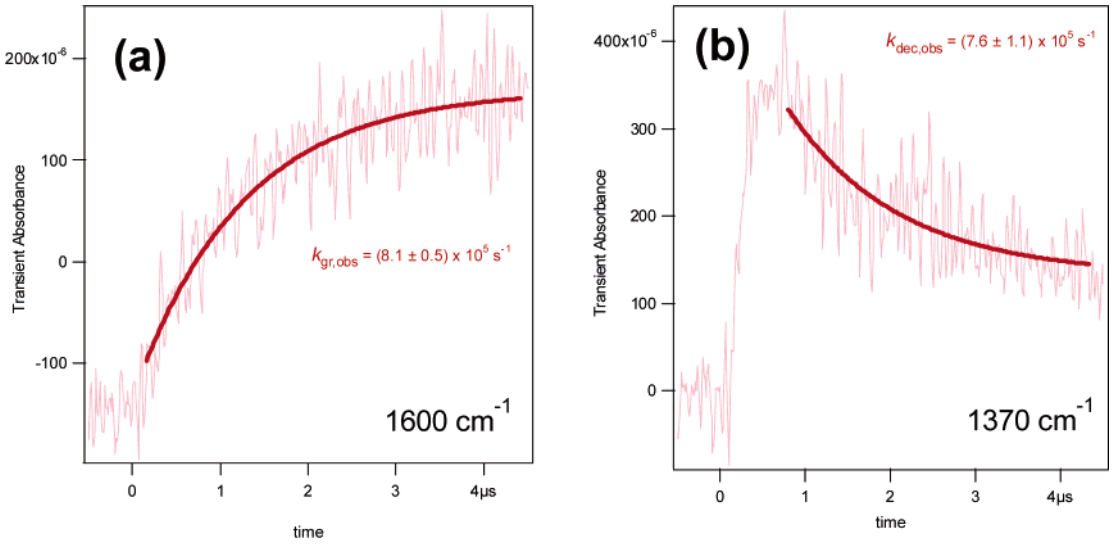

FIGURE 5. Time-resolved behavior of TRIR signals at (a) 1600 cm^{-1} and (b) 1370 cm^{-1}, following laser flash photolysis of **1** (5 mM) in d_3-acetonitrile at 298 K. The 1370 cm^{-1} signal corresponds to the triplet nitrene **3**, and the 1600 cm^{-1} signal corresponds to the azo-compound **6**.

TABLE 2. Summary of Calculated Relative Thermochemical Data (B3LYP/6-31G*, kcal/mol)

	4-nitrenopyridine-1-oxide		4-pyridylnitrene		phenylnitrene		
	B3LYP/6-31G*		B3LYP/6-31G*		B3LY P/6-31G*		CASP T2/6-31G*[a]
species	0 K[b]	298 K[c]	0 K[b]	298 K[c]	0 K[b]	298 K[c]	0 K[b]
triplet state ($^3A_2$)[d]	0.0	0.0	0.0	0.0	0.0	0.0	0.0
open-shell singlet ($^1A_2$)	9.8	9.9	16.7	16.7	15.7	15.8	19.1
closed-shell singlet ($_1A_1$)	34.4	34.3	33.1[e]	33.4[e]	47.2	47.5	37.3
singlet−benzazirine TS	34.0	33.8	33.1	32.8	31.7	31.4	27.7
benzazirine	29.7	29.7	19.7	19.7	19.9	19.8	20.7
benzazirine−ketenimine TS	36.7	36.5	21.9	21.7	23.6	23.4	25.9
ketenimine	24.3	24.2	12.7	12.7	14.7	14.8	17.8
azide singlet state (S_0)[d,f]	0.0	0.0					
azide triplet state (T_1)[f]	44.6	45.3					
N-oxide cyclization TS[f]	58.2	58.1					
cyclized *N*-oxide[f]	39.4	39.4					

[a] Ref 15. [b] Includes scaled ZPEs. [c] Includes scaled ΔH_{vib}. [d] Defined as zero. [e] This species has C_1 symmetry, therefore ^1A state. [f] Calculated relative to azide S_0 state.

oxygen onto the aromatic ring, a previously reported photochemical reaction for aromatic *N*-oxides.[20] The energetics of the open-shell singlet states of the nitrenes listed above were estimated according to the method of Johnson *et al.*,[15b] whereby a UDFT optimization based on the RDFT nitrene wavefunction with promotion of a single electron into the LUMO yielded a mixed singlet state with an $<S^2>$ expectation value of approximately 1, presumed to consist of a 50:50 mixture of open-shell singlet and triplet states. The energy of the open-shell singlet state was then estimated by the sum method (eq 1).

$$E_{(OSS)} = 2E_{(50:50\ mix)} - E_{(T)} \quad (1)$$

The results obtained for the three nitrene species are summarized in tabular form in Table 2 and in diagrammatic form in Figure 6. All energies are computed relative to the triplet ground state for each nitrene species. The thermochemical data calculated for phenylnitrene at this level of theory compares reasonably well with data generated at the CASPT2/6-31G* level of theory,[15] and so this approach should provide us with at least a qualitative (if not semiquantitative) description of the three systems.

All of the nitrene species in this study exhibit C_{2v} symmetry with the sole exception of the closed-shell singlet (S_2) state of 4-pyridylnitrene, which exhibits a single imaginary frequency under such symmetry constraints. The level of theory employed in this study indicates that this species is slightly distorted (C_1 symmetry) from a truly planar form—the potential energy well for this state is quite shallow. The other noteworthy feature of this species is that the transition state for cyclization to the benzazirine species is quite early compared to that for phenylnitrene cyclization. B3LYP/6-31G* calculations indicate that only a small deviation from planarity is required to reach the transition state. By and large, however, the energetic profiles calculated for 4-pyridylnitrene and phenylnitrene at this level of theory are quite similar. It should be noted, however, that the transition state for nitrene cyclization will retain a certain amount of biradical character that is not readily modeled by DFT methods of this type.

Consideration of *N*-oxide cyclization in **1** was considered in terms of the relative energies of the azide S_0 state and those of its cyclized intermediates (Table 2). The data indicate that such a reaction is enthalpically unfavorable to a significant degree

(20) (a) Albini, A.; Alpegiani, M. *Chem. Rev.* **1984**, *84*, 43. (b) Shi, X.; Poole, J. S.; Emenike, I.; Burdzinski, G.; Platz, M. S. *J. Phys. Chem. A* **2005**, *109*, 1491.

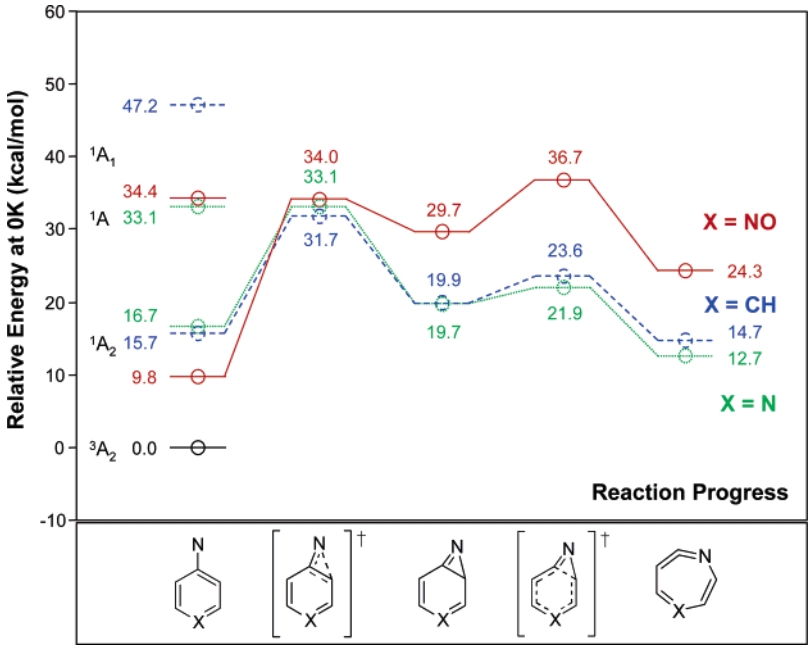

FIGURE 6. Relative energies calculated at 0 K (including ZPEs) at the B3LYP/6-31G* level of theory for the unimolecular chemistries of phenylnitrene (blue, dashed), 4-pyridylnitrene (green, dotted), and 4-nitrenopyridine-1-oxide (red, solid). All energies shown relative to the respective triplet $^3A_2$ states.

SCHEME 2. Electronic Structures of 4-Nitrenopyridine-1-oxide $^1A_2$ and $^3A_2$ States

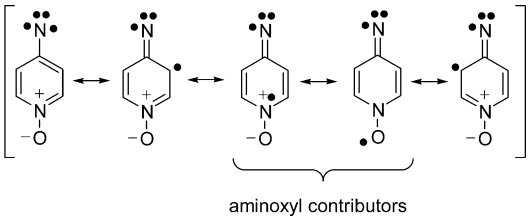

and is unlikely to occur under normal thermal conditions. Such an observation does not necessarily preclude this reaction, particularly within the photochemical realm, but it does provide additional support for the observed product distributions in this study.

Discussion

On the basis of both the observed data and previous product distribution studies, the cyclization of **2** to yield ketenimine **5** is not an energetically favorable process. In previously studied systems, this may be ascribed to steric hindrance to cyclization (e.g., *o*,*o*′-disubstituted phenylnitrenes).[21] In this particular case, no such effect is present, and so therefore we must consider the effect of electron configuration.

It is well-established that the lowest singlet state of phenylnitrene ($^1A_2$ state) is perhaps more appropriately considered as a iminyl-cyclohexadienyl biradical system[5,15] rather than a "formal" singlet nitrene. In the case of the 4-nitrenopyridine-1-oxide system, the $^1A_2$ state for **2** may be considered as an iminylaminoxyl biradical (Scheme 2), as in principle can the $^3A_2$ state of **3**.

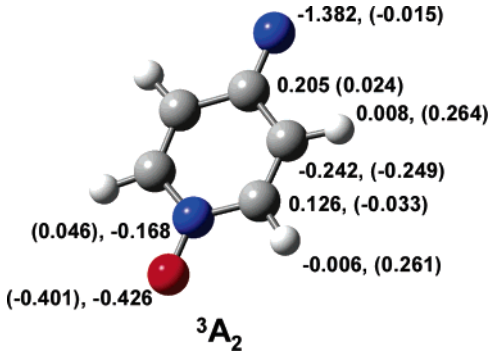

FIGURE 7. Natural population analysis of spin and charge density distribution in the $^3A_2$ state of **3**, B3LYP/6-31G* level of theory. Charge density shown in parentheses.

Given the known stability of aminoxyl radicals,[22] it is reasonable to assume that a significant amount of spin density in the ring lies on the N_1 and O atoms. A natural population analysis (NPA) was performed on the $^3A_2$ state (**3**) to obtain a measure of the spin density distribution, and the results are shown in Figure 7. The data indicate that indeed there is a significant degree of spin character on O. Such results are consistent with those previously reported by other workers.[23] On this basis, the diminution of spin density at sites *o*- to the nitreno group relative to the analogous phenylnitrene system will make cyclization a less favored process. No meaningful NPA data may be determined for the $^1A_2$ state, due to the high degree of spin contamination in the computed wavefunction,

(21) Gritsan, N. P.; Gudmundsdottir, A. D.; Tigelar, D.; Platz, M. S. *J. Phys. Chem. A* **1999**, *103*, 3458.

(22) (a) Lebvedev, Y. A.; Rosantzev, E. G.; Kalashnikova, L. A.; Lebvedev, V. P.; Neiman, M. B.; Apin, A. Y. *Dokl. Akad. Nauk SSSR* (*Engl. Trans.*) **1966**, *40*, 460. (b) Lebvedev, Y. A.; Rosantzev, E. G.; Neiman, M. B.; Apin, A. Y. *Dokl. Akad. Nauk SSSR* (*Engl. Trans.*) **1966**, *40*, 460. (c) Mahoney, L. R.; Mendenhall, G. D; Ingold, K. U. *J. Am. Chem. Soc.* **1973**, *95*, 8610.

(23) Pietrzycki, W.; Tomasik, P. *Pol. J. Chem.* **1998**, *72*, 893.

but it is reasonable to assume that the spin densities in the $^1A_2$ and $^3A_2$ would be at least qualitatively similar.

At the B3LYP/6-31G* level of theory used in this study, the singlet−triplet splitting, E_{ST}, for **2**/**3** was found to be 9.9 kcal/mol. This is some 6−7 kcal/mol smaller than those calculated for phenylnitrene and 4-pyridylnitrene. Higher level calculations at the CASSCF(10,9)/6-31G* level of theory predict E_{ST} values as low as 5.6−6.6 kcal/mol, depending on the nature of the orbitals chosen for the active space (see Supporting Information). The much smaller singlet−triplet energy gap would result in an enhanced rate of intersystem crossing observed for this species relative to phenyl nitrene, and this is observed experimentally.[24]

Upon cyclization, the stabilization afforded by additional delocalization of spin density to oxygen is lost as spin density is annihilated. The loss of this stabilizing influence upon cyclization may go part of the way to explaining why this process is much more energetically disfavored for **2** than for analogous forms: the barrier to cyclization is calculated to be 24.2 kcal/mol (ΔH_r = 19.9 kcal/mol) for **2**, but only 16 kcal/mol (ΔH_r = 3.0 and 4.2 kcal/mol) for the other systems. This level of theory tends to significantly overestimate the height of the barrier, as it both overestimates the stability of the nitrene and underestimates the stability of the transition state, which may retain significant biradical character not readily modeled by DFT methods. The CASPT2 value for the energy barrier for nitrene cyclization is 8.6 kcal/mol (the experimental value is 5.6 kcal/mol).[5c] The variation between E_{ST} calculated by DFT and CASPT2 methods is relatively systematic, and so we may conclude that the barrier to cyclization of **2** is significantly larger. It is also worth noting that the transition state for cyclization of **2** is also significantly later as might be expected from applying the Hammond postulate to Figure 6. The C−C−N angle defining the azirene ring lies between 68 and 72 for all of the benzazirine products, but is 95° in the transition state for cyclization of **2**, 105° for cyclization of phenylnitrene, and 126° for 4-pyridylnitrene.

The energetics for subsequent steps (ring-opening from benzazirine to ketenimine) is much the same for the three systems: the barriers to ring expansion vary between 2.2−7.0 kcal/mol for all three systems, and enthalpies of reaction vary between −5.2 and −7.0 kcal/mol. CASPT2 and DFT energies for the phenylnitrene system show good agreement (5.2 and 3.6 kcal/mol for the activation barrier to expansion, −2.9 and −5.2 kcal/mol for ΔH_r respectively). Once the spin density in the $^1A_2$ state is annihilated, these three systems share similar reactivity.

Formation of **6** from the triplet $^3A_2$ state of 4-nitrenopyridine-1-oxide (**3**) and parent azide (**1**) appears to be a diffusion-limited process, and so we would expect most of the complex product mixtures obtained in previous studies[3] to be the result of secondary thermal or photochemical reactions of **6**, although such product distributions may well be observable under "infinite dilution" conditions. Studies of the photochemistry of 3-azidopyridine-1-oxide and its corresponding nitrene are underway. On the basis of the arguments above, it is anticipated that this species should react more like phenylnitrene, as the positioning of the N−O group on the aromatic ring is less amenable to spin delocalization in the form of an iminyl-aminoxyl resonance contributor.

Conclusions

The photochemistry of 4-azidopyridine-*N*-oxide is dominated by fragmentation of the azide moiety—no products consistent with *N*-oxide cyclization photochemistry were observed, and calculations indicate that this process is thermodynamically disfavored. The singlet nitrene ($^1A_2$) formed undergoes rapid ISC to generate the triplet ($^3A_2$) species, which dimerizes with the azide at a diffusion-limited rate to generate the diazo-compound **6**. No singlet nitrene chemistry was observed, and calculations indicate that this is due to the significant barrier to nitrene cyclization. The barrier is significantly larger than those calculated for similar arylnitrene systems and is due to the stabilization of the $^1A_2$ and $^3A_2$ states by spin delocalization due to resonance contributors with iminyl-aminoxyl biradical character.

Acknowledgment. The authors thank Professor Matthew Platz of The Ohio State University for his gracious provision of instrument time as well as Dr. Sarah Mandel for her assistance. The authors also thank Professors Chris Hadad and William Karney for helpful discussions regarding computational methods. Calculations were made possible by use of the Beowulf cluster at the Center for Computational Nanoscience at Ball State University. Financial support in the form of a Ball State University Internal Grant and the Lilly II endowment are also gratefully acknowledged.

Supporting Information Available: Synthetic methodology for the starting material, additional spectroscopic and kinetic data obtained in this study, and computational output in the form of optimized geometries, energies, and frequencies for species relevant to this study. This material is available free of charge at http://pubs.acs.org.

JO061259O

(24) k_{ISC} for phenylnitrene is $(3.2 \pm 0.3) \times 10^6$ s^{-1} (ref 5b), close to an order of magnitude lower than the value for 4-nitrenopyridine-1-oxide. It is noteworthy that k_{ISC} may be increased three orders of magnitude with appropriate π-donor substituents (ref 6b).